

Large roots dominate the contribution of trees to slope stability

Questa è la versione Post print del seguente articolo:

Original

Large roots dominate the contribution of trees to slope stability / Giadrossich, Filippo; Cohen, Denis; Schwarz, Massimiliano; Ganga, Antonio; Marrosu, Roberto; Pirastru, Mario; Capra, Gian Franco. - In: EARTH SURFACE PROCESSES AND LANDFORMS. - ISSN 0197-9337. - 44:8(2019), pp. 1602-1609. [10.1002/esp.4597]

Availability:

This version is available at: 11388/220666 since: 2022-05-20T12:51:11Z

Publisher:

Published

DOI:10.1002/esp.4597

Terms of use:

Chiunque può accedere liberamente al full text dei lavori resi disponibili come "Open Access".

Publisher copyright

note finali coverpage

(Article begins on next page)

Large roots dominate the contribution of trees to slope stability

[Filippo Giadrossich](#), [Denis Cohen](#), [Massimiliano Schwarz](#), [Antonio Ganga](#), [Roberto Marrosu](#), [Mario Pirastru](#), [GF Capra](#)

Abstract

Tree roots provide surface erosion protection and improve slope stability through highly complex interactions with the soil due to the nature of root systems. Root reinforcement estimation is usually performed by pullout tests, in which roots are pulled out of the soil to reliably estimate the root strength of compact soils. However, this test is not suitable for the scenario where a soil progressively fails in a series of slump blocks, for example, in unsupported soils near streambanks and road cuts where the soil has no compressive resistance at the base of the hillslope. The scenario where a soil is unsupported on its downslope extent and progressively deforms at a slow strain rate has received little attention, and we are unaware of any study on root reinforcement that estimates the strength of roots in this scenario. Thus, we designed two complementary laboratory experiments to compare the pullout force of roots with and without support of colluvium at the lower extent of a hillslope. The results indicate that the root reinforcement force is reduced by up to 50% when the soil fails as slump blocks compared to pullout tests. We also found that, for slump block failure, roots had a higher tendency to slip than to break, showing the importance of active earth pressure on root reinforcement behaviour, which contributes to reduced friction between soil and roots. These results were then scaled up to a full tree and tree stand using the root bundle and field-measured spatial distributions of root density. Although effects on the force mobilized in small roots can be relevant, small roots have virtually no effect on root reinforcement at the tree or stand scale on hillslopes. When root distribution has a wide range of diameters, the root reinforcement results are controlled by large roots that hold much more force than small roots.

Introduction

Forests are part of risk reduction strategies and are an important aspect in ecosystem services (Montgomery et al., 2000; Miura et al., 2015; Moos et al., 2016; Horton et al., 2017). Among others, the effect of vegetation on slope stability is now well established (Wu et al., 1979; Gray and Lieser, 1982, Stokes et al. 2009, 2014). In addition to hydrological effects (e.g., rainfall interception and pore water pressure reduction), the main effect of vegetation on slope stability is the mechanical reinforcement of soils by roots (Sidle et al., 2006; Stokes et al., 2014; Sidle et al., 2016; Vergani et al., 2016; Sidle et al., 2017; Cohen and Schwarz, 2017; Giadrossich et al., 2017).

Three types of root reinforcement exist: basal root reinforcement, stiffening and buttressing of sliding mass under compression, and lateral root reinforcement (Vergani et al., 2017). Basal root reinforcement occurs when roots cross the shear plane and is highly efficient in stabilizing vegetated slopes. However, this type of root reinforcement occurs only in shallow soil with fractured rocks, while the shear plane of a shallow landslide occurs at depths where roots have virtually no effect (Schwarz et al., 2010a; Milledge et al., 2014). On the other hand, lateral root reinforcement has an important role but is limited depending on the area of the landslide because its contribution to slope

stability is proportionally reduced by increasing landslide size (e.g., up to 1000 m³, Schmidt et al., 2001; Schwarz et al., 2010a; Milledge et al., 2014). Nonetheless, lateral root reinforcement commonly plays a major role because shallow landslides occur more frequently (Milledge et al., 2014).

In this context, Zhou et al. (1997) were the first (and only researchers to our knowledge) to recognize the difference between two different lateral root reinforcement scenarios, i.e., roots originating from the sliding soil mass (Figure 1a) and roots originating from the stable part of a soil mass (Figure 1b, c).

Based on our direct experience, we expect a difference in root reinforcement that could differ significantly depending on the soil failure mode (Figure 1). In fact, we have observed in several landslide scarps (Figure 2) a clear indication that small roots slip while larger roots break (O'Loughlin, 1974; Gray and Barker, 2004; Pollen, 2007; Schwarz et al., 2010a). Therefore, our hypothesis is that root strength varies as a function of landslide head scarp relative to root orientation from nearby trees. Schwarz et al. (2015) showed how the unstable soil mass moving downward, acting as a wall, creates passive Earth pressure in the downslope wedge, but at the same time, it creates active pressure conditions upslope.

Active earth pressure occurs when the slide mass moves away from the roots in extension (Figure 1b, c); thus, soil disaggregates or slump blocks develop. The hypothesis is based on the fact that when the ground yields and slides downward, the downslope motion results in an increase in overall volume with a commensurate increase in void space or a decrease in bulk density. This decrease in bulk density is accompanied by a lower confining stress, hence allowing a higher amount of root slippage within the expanded mass. Therefore, the rheology of the mass of ground in the landslide leads to a low frictional resistance between the soil and root because the contact between the root and soil has a low confining stress.

In contrast, in practice, root reinforcement is measured by extracting the roots (pullout tests) from a completely stable and aggregated soil (Giadrossich et al., 2017). This method by Zhou is as follows: i) classic root extraction tests measure the root reinforcement and ii) soil disaggregation tests measure conditions that would lead to a reduction in root reinforcement (with respect to the pullout tests). These two cases are represented by Figures 1a and 1b, c, respectively.

Pullout tests are one of the most used and important direct tests to assess root reinforcement (Giadrossich et al., 2017); nonetheless, this type of test represents root extraction from a stable soil, analogous to the scenario where a shallow landslide initiates uphill with respect to the trees. This scenario is rarely encountered in reality: most often, trees are upslope of the tension crack. By analogy, this latter scenario is similar to the cases of forest clear-cuts, riverbanks, and road cuts (Figure 1b, c).

To elucidate the active earth pressure role on root reinforcement mechanisms, we performed original and systematic measurements of root reinforcement in the laboratory using a device on a tiltable plane where the soil containing the roots was placed to simulate a landslide. Then, we performed classic pullout tests (Giadrossich et al., 2017). Our objective is to quantify the difference in root reinforcements between the two hillslope configurations with respect to tree position described in Zhou et al. (1997). Finally, for a case study, we calculated the root reinforcement using the root bundle model (RBMw) (Schwarz et al., 2013), considering the findings of this research.

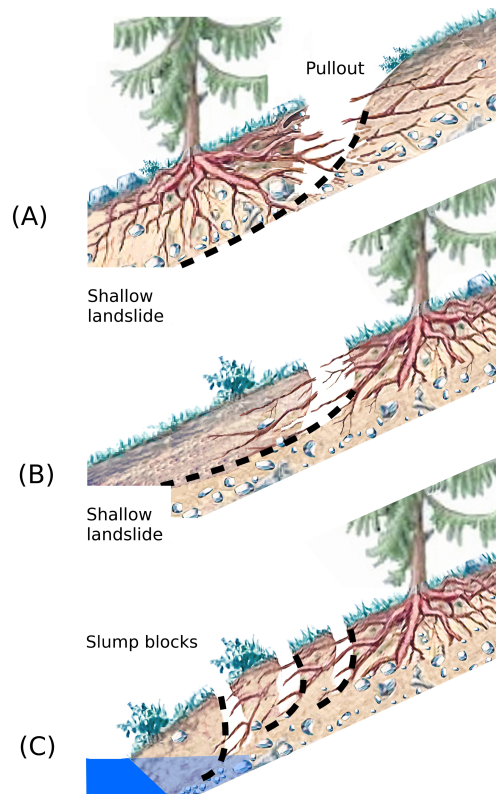


Figure 1: Schematic illustration of the different hillslope configurations with respect to tree position: (a) roots anchored in the sliding mass across a tension crack. Passive soil strength can develop at the toe, while stiffening and buttressing by roots in the soil mass may occur; (b) roots coming from the stable mass; and (c) roots coming from the stable mass with multiple slump block failures. Cases (b) and (c) consider the topographic context of an abrupt slope decrease at the hillslope base with an accommodation space for slide material to move into, analogous with road margins and riverbanks. The black dotted line indicates the shear plane.

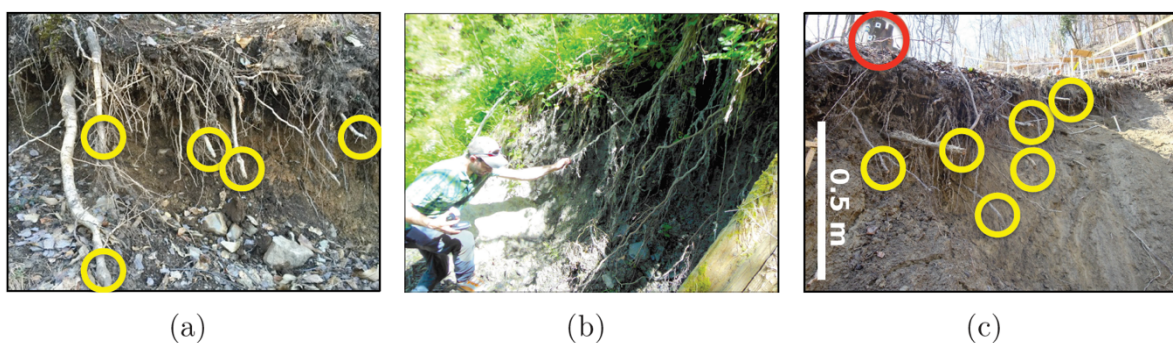


Figure 2: Most broken roots are large, while small roots remain intact, indicating slippage. (a) Landslide scarp with protruding roots (yellow circles) in a chestnut forest (Italy, photo by Andrea Dani). (b) Landslide scarp with protruding roots in a mixed broadleaf and conifer forest stand (Switzerland, photo by Filippo Giadrossich). (c) Landslide scarp with protruding roots (yellow circles) in an *Aceri-Fraxinetum* forest stand (Switzerland, photo by Massimiliano Schwarz). The red circle indicates the position of a tree stump.

Root-soil friction model

The force activated along a root depends on root-soil friction, which is given by the root frictional shear stress times the root-soil area of contact, approximated as the root length times the root average perimeter. The maximum frictional shear stress reached by the root can be calculated assuming Coulomb failure (Schwarz et al. 2010c), i.e.,

$$T = c_r + \mu\sigma'$$

where c_r is apparent cohesion, μ is the friction coefficient between the soil and the root and is assumed to be uniform along the root length and perimeter, and σ' is the normal stress. The normal stress is obtained by multiplying the vertical stress by the cosine of the inclination angle. The friction coefficient μ includes the effects of root shape, tortuosity, and branching.

Root Bundle Model

To estimate the effects of lateral earth pressure on root reinforcement, we estimate root reinforcement using the RBMw (Schwarz et al. 2013) using data from our two laboratory experiments. The general equation to calculate root reinforcement (F) of a bundle of roots as a function of displacement is

$$F_{tot}(x) = \sum_{i=1}^N F(\phi_i, x) S(\xi_i),$$

where N is the total number of roots, x is the displacement (i.e., how much the roots stretch across the tension gap), $S(\xi_i)$ is the survival function assumed to have a Weibull distribution, ξ_i is normalized displacement, and ϕ_i is the size of root diameter class i . The RBMw assumes no interaction between neighbouring roots or crossing roots (Giadrossich et al., 2013). Details of the model and methodology can be found in Schwarz et al. (2013) and Giadrossich et al. (2016).

Materials and methods

Soil and roots

The soil sample used for the experiments was a sandy loam soil collected in Nuoro Province (Sardinia, Italy). Soil physical analyses were carried out on air-dried soil samples (fraction <2 mm) in accordance with official Italian procedures (MiPAF, 2000) and in compliance with international standards. Sand (2.0-0.02 mm), silt (0.02-0.002 mm), and clay (<0.002 mm) fractions were separated by pipette and wet sieving following pretreatment with H_2O_2 and sodium hexametaphosphate. Textural classes were identified according to the USDA (Soil Survey Laboratory Staff, 2014). Soil

cohesion and friction angle were obtained by extrapolation from failure points obtained by direct shear tests with normal stress values of 2.7, 6.0, and 12 kPa and fitted by a linear regression (Giadrossich et al., 2017). The normal stress used was lower than that in the classic geotechnical direct shear test because the magnitude of the normal stress at the failure surface of shallow landslides is only a few kPa. The physical properties of the soils used in the experiments are reported in Table 1.

Table 1: Particle size and geotechnical parameters of soils.

Soil type	VWC [%]	Sand [%]	Silt [%]	Clay [%]	Effective cohesion c' [KPa]	Friction angle ϕ [degree]
Sandy loam	27	80	9	11	23.47	39.21

Roots of *Pseudotsuga menziesii* (Mirb.) Franco (Douglas fir) were collected from the centre of Sardinia, Italy. The roots were dug by hand, and then the length and diameter at both extremities were measured. The root diameters ranged from 2 to 10 mm, with lengths between 0.52 and 1.65 metres.

Slump blocks and pullout: experimental setup

To perform our tests, we needed to build a tiltable plane to place the soil containing the roots. In one case, we measured the force needed to extract the roots, and we named these experiments "pullout". This case relates to the study of the dynamics described in Figure 1a. In the other case, we measured the force applied to the roots from the soil that is slipping, simulating a landslide. The latter tests are called "slump blocks", referring to the type of soil behaviour under active earth pressure (Figure 1b, c).

We designed a tilting box to perform both slump block and pullout experiments in the laboratory. The tilting box (Figure 3), 0.8 m wide, 1.5 m long, and 0.5 m high, is delimited by 3 fixed pieces of plywood, two on the sides and one upslope, which contain the soil sample and the roots. The upslope side has holes through which roots are anchored to load cells attached to a movable plywood panel sliding along rails with ball bearings (red and orange lines in Figure 3). The plywood panel holds up to fifteen load cells (Omega Inc. LCL-040, maximum load 180 N). The box is mounted on a platform that can be tilted 45 degrees from horizontal using a hydraulic jack.

For the pullout experiments, the movable side panel pulls the roots (Figure 3) by loading weights onto a frame attached to the side panel through a steel cable. For the slump block experiments, the roots are connected to the load cells that measure the tensional force in the roots when soil slips past them when the box is tilted (Figure 3). In this case, the movable side remains fixed and acts as an anchor point for the roots.

Preparation of the rooted soil followed a strict procedure. Successive strata of soil were laid out in the box, and roots were inserted between strata until the soil was 0.45 m deep. The roots were inserted at three different levels, 0.10, 0.25, and 0.40 m from the bottom of the box. The roots extended a few centimetres into holes in the wooden movable side and were each connected to a load cell. The load cells were connected to a data logger for continuous recording of data. The sampling rate was 1 Hz. The roots were reused in both slump block and pullout experiments unless they broke. In this case, they were replaced with roots of similar diameter and length.

For all experiments, the soil moisture ranged between 27 and 29%. A total of 92 single roots were tested in 8 experiments.

Then, to upscale the root reinforcement calculation, we first surveyed the root distribution in the field for 5 different trees, digging two trenches of 0.6 m² for each tree at two different distances from the trunk (for details, see Schwarz et al., 2012). Then, the root distribution was estimated at other distances using the model by Schwarz et al. (2012), as described in Giadrossich et al. (2016). The model estimates the number of roots for each 1 mm diameter class in a vertical section of 1 m² as a function of the distance from the tree trunk.

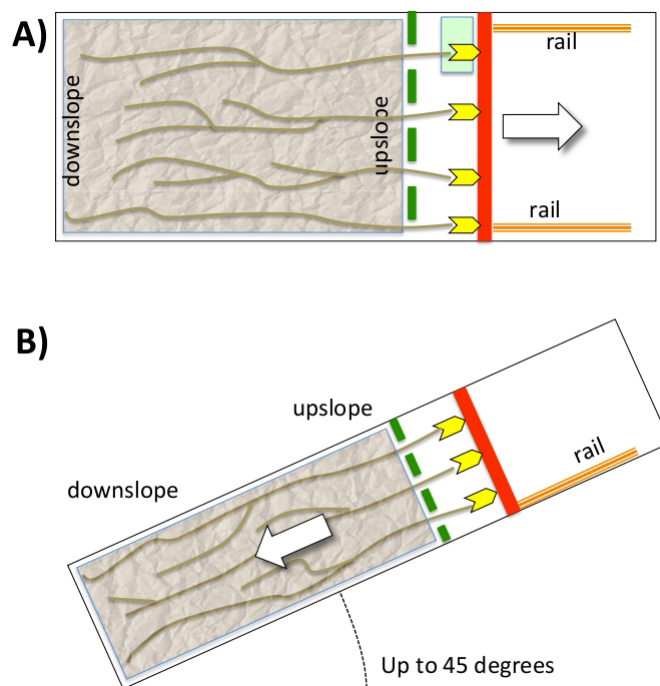


Figure 3: Schematic of the tilting box: A) plan view and B) lateral view. The red bold line represents the plywood panel that moves along the rails and pulls the roots to reproduce roots being pulled out by the downslope tree (reproducing the scenario in Figure 1a). This panel carries the load cells. The dotted line represents the fixed plywood panel that protects the load cells and data loggers. The roots pass through this panel to be anchored to the load cells on the movable side (bold red line). The tilting box can be inclined up to 45 degrees, allowing the soil to slip and reproducing the active earth pressure on roots (the scenario in Figure 1b, c).

Statistical analysis

To analyse the data, we performed an analysis of covariance (ANCOVA) using a two-level factor (force recorded on the roots) and a continuous covariate parameter (normal stress) and Student's t-test. Normal stress was scaled as a function of tilting angle to obtain a comparable setup between the experiments. All statistical analyses were carried out using the statistical software R 3.2.1 (R Development Core Team, 2015).

Results

Figure 4 shows the effect of normal stress (σ') on the maximum friction stress (T , see Eq. 1) for the two types of experiments, pullout and slump blocks. For a given normal stress, the data are highly scattered, and no apparent trend appears with normal stress.

Statistical analysis showed that in our case, normal stress has no effect on the maximum friction stress (see Table 2 in the appendix). This result also confirms the hypothesis, which is commonly not taken into consideration, that the inclination angle of the slope does not influence the frictional shear stress between the root and soil, and thus, normal stress correction is entirely neglected.

Student's t-test indicated, however, that the friction shear stress was significantly higher in the pullout experiments (mean= 4.46 ± 1.04 kPa) than in the slump block experiments (mean= 2.11 ± 0.57 kPa), $p < 0.001$, at the 95% confidence level. Figure 5 graphically shows the relationship of the two experiments. The results are significantly different ($p < 0.001$).

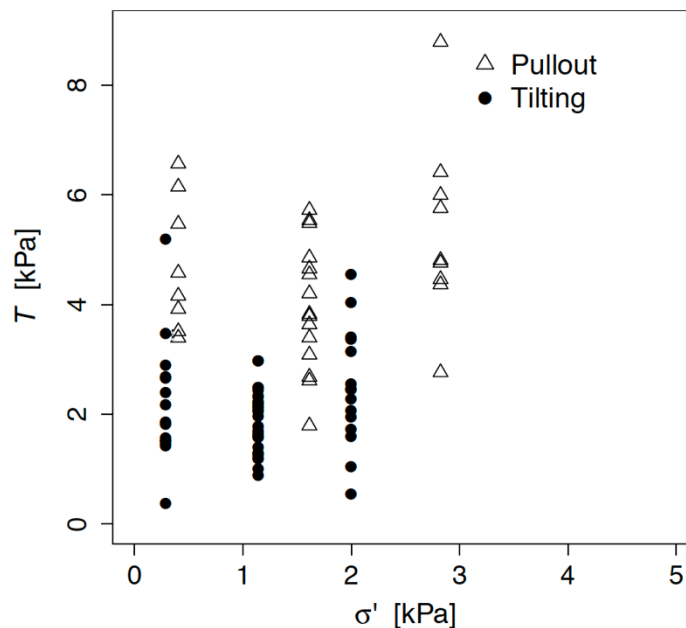


Figure 4: Effect of variation in normal stress (σ') on the maximum friction stress. The normal stresses between pullout experiments and tilting experiments differ because of the slope angle correction.

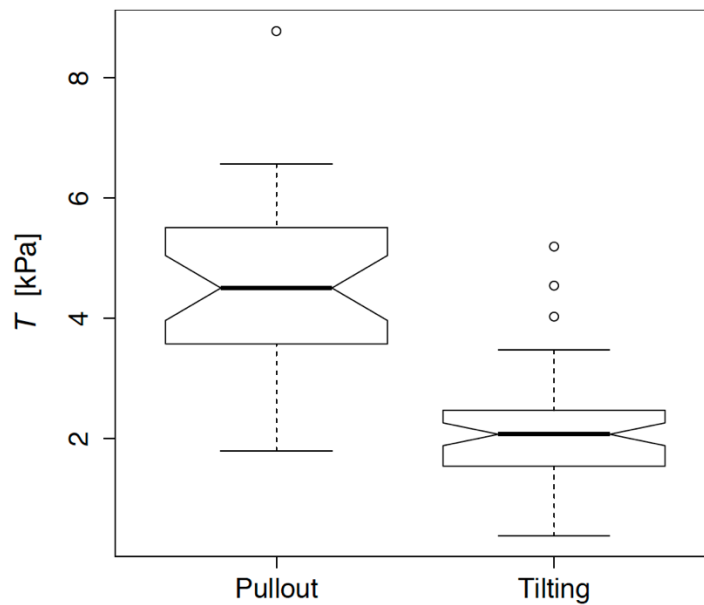


Figure 5: Boxplot showing the median, first and third quartiles, and maximum and minimum values of root friction shear stress for the pullout and tilting experiments.

Discussion

The range of normal stress values in the experiment does not justify the different values of frictional stress (T) recorded. Thus, the changes in T are due to the apparent cohesion term (c), which summarizes the results for the two experiments, suggesting that soil-root cohesion forces are lower for the slump block experiments due to the active earth pressure. We observe that in the slump block experiments (tilting box), soil slip induces tensile strain inside the soil, which is also due to the presence of roots, breaking up the soil aggregates and structure and reducing the soil-root contact area and soil-root cohesion. Again, the active earth pressure represents the extensional case where slump blocks develop, resulting in a general decrease in volume and compressive stress and increasing the likelihood that roots will slip and not break. As a result, more roots slipped in the experiments, resulting in overall less mobilized force, up to 50% less with respect to the pullout experiments.

Confining pressure and root size (the latter is proportional to the root length and number of branches) are the driving factors. Small roots, at such small confining pressure, cannot exceed the length criterion (Waldron, 1977), i.e., roots do not exceed the critical length imbedded into the soil that is required to break them. The results are similar to those of Schwarz et al. (2011), where for normal stress ranging from 2 to 4.5 kPa, these authors found little variation in the maximum pullout force.

Soil type could have an important impact. A more cohesive soil could increase root-soil bond forces (e.g., Schwarz et al. 2011) and mobilize more force during the experiments. This result would lead to a smaller difference between the forces activated during pullout or slump block setups. Soil saturation, however, could have a reversal effect. Higher saturation along streambanks would reduce cohesive forces due to suction, increasing the difference between root reinforcement on river banks and road cuts or vegetated slopes.

The laboratory tests we have performed certainly represent a simplified system. However, soil environment tests in the field can sometimes be difficult to set up due to the particularity of these tests and the many variables considered. For these reasons, simplified systems are preferable to study. Examples are studies of the effect of root tortuosity, the weight of the soil, the type of soil, and so on, e.g., Mickovski et al. (2009), Schwarz et al. (2010), and Giadrossich et al. (2013). The results we obtained from these tests, however, confirm our field observations made on the detachment niche of numerous landslides, where the large roots are broken, extending out for a certain length, while the numerous fine roots (up to three millimetres) mainly slip out without breaking. However, other authors have made similar observations.

Pollen et al. (2005) observed that the roots of river birch (*Betula nigra* L.) smaller than 3.5 mm would slip out, while larger roots would break. Schwarz et al. (2010b), using a discrete element model for single roots that included root-soil and branching friction, also showed that small roots of spruce (*Picea abies* L.) would tend to slip, while large roots would break. Zhou et al. (1997) carried out *in situ* experiments of pulling soil cuboids containing roots of *Pinus yunnanensis* (Franch.), indicating that roots greater than 3 mm tend to break. Additionally, Schmidt et al. (2001), in a detailed survey of landslide scarps in Oregon, USA, found a large majority of broken roots, although no indication was given as to their sizes.

The difference between active earth pressure and pullout from stable soil is not one of merely a change in the frame of reference but a completely distinct failure mode that will activate different forces along roots. Different force activations due to frictional root-soil contact will dictate whether roots slip or break during soil motion. The substantial significance of these results lies in the fact that root reinforcement in the distal areas of trees decreases more rapidly than we might expect. Thus, when there is a tree at the top of a slope, as in the case of road embankments, riverbanks, or even hill slopes, the downward root reinforcement is reduced as a function of root distribution in the soil. If large roots are present, this reduction can be ignored because the large roots support the overwhelming majority of the forces at stake. If only fine roots are present, a reduction of up to 50% of the root reinforcement can occur. The reason lies in the fact that in the latter case, most of the roots slip out rather than break. Thus, we infer that during landslide initiation, large-diameter roots may share the load with the small-diameter roots until the small-diameter roots slip out, at which time soil may slip along the large-diameter roots until they break.

The root reinforcement reduction described in this article should not be confused with the well-known overestimation of root reinforcement when calculated with the so-called Wu model (Wu, 1979; Waldron et al. 1981) or the RipRoot Model by Pollen et al. (2004) due to incorrect assumptions on root breaking dynamics (Abernethy and Rutherford, 2000, 2001; Simon and Collison, 2002; Pollen and Simon, 2005; Docker2008, Pollen2009, Hubble2010, Schwarz2013).

Despite the limits of experimentation in the laboratory, a new method was applied, and a rigorous experimental protocol was followed. The only way to perform such tests in the field would be to artificially trigger a landslide, where the roots were previously connected to load cells. This approach is undoubtedly very stimulating but also very expensive and complicated. For instance, a large-scale artificial rainfall-induced landslide triggering experiment was performed in Spring 2009 in Switzerland (Schwarz et al., 2012), but unfortunately, no direct measurement of the force applied on the roots was taken.

The slippage of small roots is never considered in the literature of root reinforcement models. Root reinforcement calculations are still based on the assumption that all roots break. Model calibration is performed using data obtained usually by laboratory tensile strength or field root pullout (e.g., Giadrossich et al., 2017; Tosi, 2007; Docker and Hubble, 2008; Genet et al., 2008; Hales et al., 2009; Cohen et al., 2011; Mao et al., 2012). In the following section, we carried out simulations to assess the impact of small roots on root reinforcement on the basis of our findings applied to original data of root distributions and root pullout tests of Douglas fir.

Application

We consider three scenarios: (i) the root strength is given by field pullout measurements (all roots fail under tension, Figure 1a); (ii) the strength of roots less than or equal to 6 mm is reduced by 50% based on our laboratory results (Figure 1b) (similar to Pollen et al., 2005); and (iii) the strength of all roots is reduced by 50% (Figure 1c). The root reinforcement for these scenarios is calculated using the RBMw.

Figure 5 shows root reinforcement as a function of displacement (soil slippage) for these three scenarios. For distances of 0.75 and 1.5 metres from the trunk, the effect of a reduced breaking force for roots less than 6 mm (scenario (ii)) is limited in magnitude and affects only the first few decimetres of displacement (see the difference between the solid and dashed curves in Figure 5). This effect does not affect the value of maximum root reinforcement because maximum root reinforcement occurs at a displacement where these small roots no longer hold any force. In contrast, at 2.25 metres from the stem, peak root reinforcement occurs at a smaller displacement, and the maximum force is reduced by 50%. Root reinforcement near the tree trunk is controlled by many large roots. The contribution to root reinforcement for roots less than 6 mm is minimal. In contrast, far from the tree trunk, coarse roots are minimal, and roots smaller than 6 mm contribute significantly to the total root reinforcement.

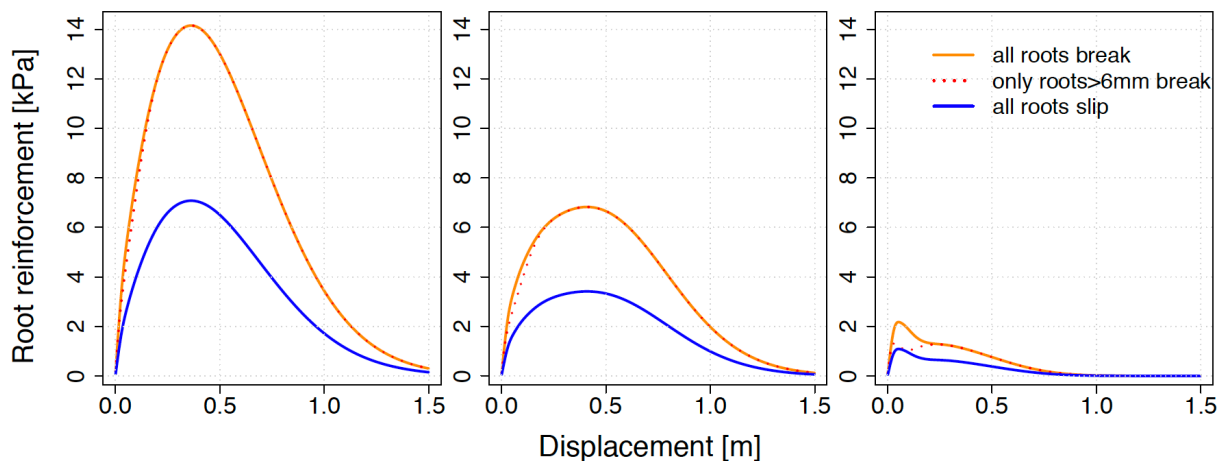


Figure 5: Root reinforcement as a function of displacement calculated at (a) 0.75 metres, (b) 1.5 metres, and (c) 2.25 metres from the stem for the three scenarios ((i) to (iii)) described in the main text. The RBMw parameters are $F_0=0.620 \times 10^6$, $k_0=0.210 \times 10^6$, $\alpha=1.60$, $\beta=0.96$, $\omega=2.4$, and $\lambda=1$ obtained from field pullout tests (for more details, see Schwarz2013, Giadrossich2016).

A last consideration must be made based on the fact that the largest decreases in root reinforcement occur where only small roots are present, and therefore, the reduction in root reinforcement takes place on already relatively low resistance values. Therefore, these findings have an effect depending on the root distribution and size of shallow landslides.

Conclusions

Most research on the effect of vegetation on slope stability does not consider the two end-member anchoring scenarios described in Zhou et al. (1997). These different anchoring scenarios and their effects on root reinforcement were estimated in laboratory experiments and filled a gap in the literature.

In the dynamics of root reinforcement during landslide initiation, large-diameter roots may share the imposed load with small-diameter roots until the small-diameter roots break, at which time soil may slip along the large-diameter roots.

The results confirm the experimental hypothesis, showing an average difference of approximately 50% between the pullout force and the force exerted on the roots when the soil fails in progressive blocks. For stiff, large soil movement, this difference is drastically reduced and is entirely neglected when large roots are present in the soil because large roots mobilize most of the force. Thus, root size distribution is fundamental to make accurate predictions of root reinforcement. The effect of root slippage is important whenever root distribution is limited to minimal and small-diameter classes. Considering the implication for bioengineering work, root reinforcement calculations on short and steep slopes, such as riverbanks and roadcuts, can be lower than expected. In comparison to the model by Wu et al. (1979), which is still commonly used for estimating root reinforcement, our results indicate that the reduction in root reinforcement is on the order of 75% when all roots crossing a soil profile are small. For this reason, we advise against the use of the model by Wu et al. (1979), and we suggest the use of models based on more realistic interactions between roots and soil, such as the root bundle model (Schwarz et al., 2013).

Appendix

Table 2 shows the analysis of variance output of the fitted model. Normal stress does not show any effect ($p=0.347$) on the response variable (T). Explanatory variables do not show any interaction or any difference between the two slopes of this relationship ($p>0.05$). This result can be better observed in Figure 4, where all the data have been plotted as a function of the type of experiment and normal stress. The active earth pressure has a highly significant effect on friction shear stress ($p<0.001$). Consequently, we considered only the minimal model “pullout” versus “slump block” experiments to be valid.

Table 2: Analysis of variance with friction shear stress as a response. Df, degree of freedom; Sum Sq, sum of squares.

	Df	Sum Sq	Mean Sq	F value	Pr(>F)
Pull:Slump	1	33.05	33.05	45.60	0.0000
Normal stress	1	0.93	0.93	1.28	0.2709
Pull-Slump:Normal stress	1	0.07	0.07	0.10	0.7581
Residuals	20	14.50	0.72		

Acknowledgements

We thank the Consorzio Universitario di Nuoro and Dr. Massimo D'Angelo of Agenzia Fo.Re.S.T.A.S. for his help and support. We also thank Francesco Lai and Matteo Urru from the University of Sassari for their help in the field. Dr. Denis Cohen was supported by funds from the Visiting Professor Program of the University of Sassari.

Abernethy B, Rutherford ID. 1998. Where along a river's length will vegetation most effectively stabilise stream banks?. *Geomorphology* 23:55–75. DOI:10.1016/S0169-555X(97)00089-5

Abernethy B, Rutherford ID. 2000. The effect of riparian tree roots on the mass-stability of riverbanks. *Earth Surface Processes and Landforms* 25:921-937. DOI:10.1002/1096-9837(200008)25:9<921::AID-ESP93>3.0.CO;2-7

Abernethy B, Rutherford ID. 2001. The distribution and strength of riparian tree roots in relation to riverbank reinforcement. *Hydrological Processes* 15(1):63-79

Beeson CE, Doyle PF. 1995. Comparison of bank erosion at vegetated and non-vegetated channel bends. *Journal of the American Water Resources Association* 31(6):983-990. DOI:10.1111/j.1752-1688.1995.tb03414.x

Cohen D, Schwarz M, Or D. 2011. An analytical fiber bundle model for pullout mechanics of root bundles. *Journal of Geophysical Research* 116, F03010. DOI:10.1029/2010JF001886

Cohen D, Schwarz M. 2017. Tree-roots control of shallow landslides. *Earth Surface Dynamics*. DOI:10.5194/esurf-5-451-2017

Dapporto S, Rinaldi M, Casagli N, Vannocci P. 2003. Mechanisms of riverbank failure along the Arno River, central Italy. *Earth Surface Processes and Landforms* 28(12):1303-1323. DOI:10.1002/esp.550

Docker BB, Hubble TCT. 2008. Quantifying root-reinforcement of river bank soils by four Australian tree species. *Geomorphology* 100(3):401-418. DOI:10.1016/j.geomorph.2008.01.009

Genet M, Kokutse N, Stokes A, Fourcaud T, Cai X, Ji J, Mickovski S. 2008. Root reinforcement in plantations of *Cryptomeria japonica* D. Don: effect of tree age and stand structure on slope stability. *Forest Ecology and Management* 256:1517–1526. DOI:10.1016/j.foreco.2008.05.050

Giadrossich F, Schwarz M, Cohen D, Preti F, Or D. 2013. Mechanical interactions between neighbouring roots during pullout tests. *Plant and soil* 367(1-2):391-406. DOI:10.1007/s11104-012-1475-1

Giadrossich F, Cohen D, Schwarz M, Seddaiu G, Contran N, Lubino M, Valdés-Rodríguez OA, Niedda M. 2016. Modeling bio-engineering traits of *Jatropha curcas* L.. *Ecological Engineering* 89:40-48. DOI:10.1016/j.ecoleng.2016.01.005

Giadrossich, F., Schwarz, M., Cohen, D., Cislighi, C., Vergani, C., Hubble, T., Phillips, C., Stokes, A. (2017). Methods to measure the mechanical behaviour of tree roots: A review. *Ecological Engineering* 109(B):256-271. DOI:10.1016/j.ecoleng.2017.08.032

Gray DH, Leiser AT. 1982. Biotechnical slope protection and erosion control. Van Nostrand Reinhold Company Inc., New York.

Gray DH, Barker D. 2004. Root-Soil Mechanics and Interactions. In: Riparian Vegetation and Fluvial Geomorphology (eds S.J. Bennett and A. Simon), American Geophysical Union, Washington, D.C.. DOI:10.1029/008WSA09

Hales TC, Ford RC, Hwang T, Vose JM, Band LE. 2009. Topographic and ecologic controls on root reinforcement. *Journal of Geophysical Research* 114. DOI:10.1029/2008JF001168

Horton AJ, Constantine JA, Hales TC, Goossens B, Bruford MW, Lazarus ED. 2017. Modification of river meandering by tropical deforestation. *Geology* 45(6):511-514.

Hubble TCT, Docker BB, Rutherford ID. 2010. The role of riparian trees in maintaining riverbank stability: a review of Australian experience and practice. *Ecological Engineering* 36(3):292-304. DOI:10.1016/j.ecoleng.2009.04.006

Mao Z, Jourdan C, Bonis ML, Pailler F, Rey H, Saint-Andr e L, Stokes A. 2012. Modelling root demography in heterogeneous mountain forests and applications for slope stability analysis. *Plant and Soil* 363(1-2):357-382. DOI:10.1007/s11104-012-1324-2

Miura S, Amacher M, Hofer T, San-Miguel-Ayanz J, Thackway R. 2015. Protective functions and ecosystem services of global forests in the past quarter-century. *Forest Ecology and Management* 352:35-46. DOI:10.1016/j.foreco.2015.03.039

Moos C, Bebi P, Graf F, Mattli J, Rickli C, Schwarz M. 2015. How does forest structure affect root reinforcement and susceptibility to shallow landslides?. *Earth Surface Processes and Landforms* 41:951-960. DOI:10.1002/esp.3887

Montgomery DR, Schmidt KM, Greenberg HM, Dietrich WE. 2000. Forest clearing and regional landsliding. *Geology* 28(4):311-314. DOI:10.1130/0091-7613(2000)28<311:FCARL>2.0.CO;2

O'Loughlin CL. 1974. A study of tree root strength deterioration following clearfelling. *Canadian Journal of Forest Research* 4(1):107-113. DOI:10.1139/x74-016

Pollen N, Simon A, Collison A. 2004. Advances in assessing the mechanical and hydrologic effects of riparian vegetation on streambank stability. in: Riparian Vegetation and Fluvial Geomorphology (eds S. J. Bennett and A. Simon), American Geophysical Union, Washington D.C.. DOI:10.1029/008WSA10

Pollen N, Simon A. 2005. Estimating the mechanical effects of riparian vegetation on stream bank stability using a fiber bundle model. *Water Resources Research* 41(7), W07025. DOI:10.1029/2004WR003801

Pollen N. 2007. Temporal and spatial variability in root reinforcement of streambanks: accounting for soil shear strength and moisture. *Catena* 69(3):197-205. DOI:10.1016/j.catena.2006.05.004

Pollen-Bankhead N, Simon A, Jaeger K, Wohl E. 2009. Destabilization of streambanks by removal of invasive species in Canyon de Chelly National Monument, Arizona. *Geomorphology* 103(3):363-374. DOI:10.1016/j.geomorph.2008.07.004

R Development Core Team (2015). R: A Language and Environment for Statistical Computing
R Foundation for Statistical Computing URL, Viena, Austria (2015) <http://www.R-project.org>

Milledge DG, Bellugi D, McKean JA, Densmore AL, Dietrich WE 2014. A multidimensional stability model for predicting shallow landslide size and shape across landscapes. *Journal of Geophysical Research: Earth Surface*, 119(11), 2481-2504.

Nardi L, Rinaldi M, Solari L. 2012. An experimental investigation on mass failures occurring in a riverbank composed of sandy gravel. *Geomorphology*, 163:56-69.
DOI:10.1016/j.geomorph.2011.08.006

Schwarz M, Preti F, Giadrossich F, Lehmann P, Or D. 2010. Quantifying the role of vegetation in slope stability: a case study in Tuscany (Italy). *Ecological Engineering*, 36(3):285-291.
DOI:10.1016/j.ecoleng.2009.06.014

Schwarz, M., Lehmann, P., and Or, D. 2010b. Quantifying lateral root reinforcement in steep slopes from a bundle of roots to tree stands. *Earth Surface Processes and Landforms*, 35-3, 354-367.
DOI:10.1016/j.ecoleng.2009.06.014

Schwarz M, Cohen D, Or D. 2010c. Soil-root mechanical interactions during pullout and failure of root bundles. *Journal of Geophysical Resources* 115, F04035. DOI:10.1029/2009JF001603.

Schwarz M, Cohen D, Or D. 2011. Pullout tests of root analogs and natural root bundles in soil: Experiments and modeling. *Journal of Geophysical Research* 116, F02007.
DOI:10.1029/2010JF001753

Schwarz M, Cohen D, Or D. 2012a. Spatial characterization of root reinforcement at stand scale: Theory and case study. *Geomorphology* 171-172:190-200. DOI:10.1016/j.geomorph.2012.05.020

Schwarz M, Giadrossich F, Cohen D. 2013. Modeling root reinforcement using a root-failure Weibull survival function. *Hydrology and Earth System Sciences*, 17(11):4367-4377.
DOI:10.5194/hess-17-4367-2013

Schwarz, M., Rist, A., Cohen, D., Giadrossich, F., Egorov, P., Büttner, D., Stolz, M, Thormann, J.-J. (2015). Root reinforcement of soils under compression. *Journal of Geophysical Research: Earth Surface*, 120(10), 2103-2120.

Schmidt KM, Roering JJ, Stock JD, Dietrich WE, Montgomery DR, Schaub T. 2001. The variability of root cohesion as an influence on shallow landslide susceptibility in the Oregon Coast Range. *Canadian Geotechnical Journal* 38:995-1024. DOI:10.1139/t01-031

Sidle RC, Ochiai H. 2006. Landslides: processes, prediction, and land use. *Water Resources Monograph* 18, American Geophysical Union (AGU), Washington, D.C., USA.

Sidle RC, Bogaard TA. 2016. Dynamic earth system and ecological controls of rainfall-initiated landslides. *Earth-Science Reviews* 159:275–291. DOI:10.1016/j.earscirev.2016.05.013

Sidle RC, Ziegler AD. 2017. The canopy interception-landslide initiation conundrum: insight from a tropical secondary forest in northern Thailand. *Hydrology and Earth System Sciences*, 21(1):651-667.

\bibitem[Soil Survey Laboratory Staff(2004)]{SoilSurveyLaboratoryStaff2014}
Soil Survey Laboratory Staff (2004). Soil Survey Laboratory Methods Manual. Soil Survey Investigations Report, vol. 42. National Soil Survey Center, Lincoln, NE Version 4.0. USDA-NRCS.

Simon A, Collison AJ. 2002. Quantifying the mechanical and hydrologic effects of riparian vegetation on streambank stability. *Earth Surface Processes and Landforms* 27(5):527-546.
DOI:10.1002/esp.325

Stokes A, Atger C, Bengough AG, Fourcaud T, Sidle RC. 2009. Desirable plant root traits for protecting natural and engineered slopes against landslides. *Plant and Soil* 324(1-2):1-30.
DOI:10.1007/s11104-009-0159-y

Stokes A, Douglas GB, Fourcaud T, Giadrossich F, Gillies C, Hubble T, John HK, Kenneth WL, Zhun M, McIvor IM, Mickovski SB, Mitchell S, Osman N, Phillips C, Poesen J, Polster D, Preti F, Raymond P, Rey F, Schwarz M, Walker LR, Mickovski SB. 2014. Ecological mitigation of hillslope instability: ten key issues facing researchers and practitioners. *Plant and Soil*, 377(1-2):1-23. DOI:10.1007/s11104-014-2044-6

Tosi M. 2007. Root tensile strength relationships and their slope stability implications of three shrub species in the Northern Apennines (Italy). *Geomorphology* 87:268–283.
DOI:10.1016/j.geomorph.2006.09.019

Vergani, C., Schwarz, M., Soldati, M., Corda, A., Giadrossich, F., Chiaradia, E. A., Morando, P., Bassanelli, C. (2016). Root reinforcement dynamics in subalpine spruce forests following timber harvest: a case study in Canton Schwyz, Switzerland. *Catena*, 143, 275-288.
DOI:10.1016/j.catena.2016.03.038.

Vergani C, Giadrossich F, Buckley P, Conedera M, Pividori M, Salbitano F, Lovreglio R, Schwarz M. 2017. Root reinforcement dynamics of European coppice woodlands and their effect on shallow landslides: A review. *Earth-Science Reviews* 167:88-102. DOI:10.1016/j.earscirev.2017.02.002.

Waldron LJ, Dakessian S. 1981. Soil reinforcement by roots: calculation of increased soil shear resistance from root properties. *Soil Science* 132(6):427-435.

Wu TH, McKinnell WP, Swanston DN. 1979. Strength of tree roots and landslides on Prince of Wales Island, Alaska. *Canadian Geotechnical Journal* 16:19-33. DOI:10.1139/t79-003

Zhou Y, Watts D, Cheng X, Li Y, Luo H, Xiu Q. 1997. The traction effect of lateral roots of *Pinus yunnanensis* on soil reinforcement: a direct in situ test. *Plant and Soil* 190(1):77-86.
DOI:10.1023/A:1004263205165

Zhou Y, Watts D, Li Y, Cheng X. 1998. A case study of effect of lateral roots of *Pinus yunnanensis* on shallow soil reinforcement. *Forest ecology and Management* 103(2-3):107-120.
DOI:10.1016/S0378-1127(97)00216-8.